Dopamine Blocks Stress-Mediated Ovarian Carcinoma Growth

Myrthala Moreno-Smith[1], Chunhua Lu[1], Mian M.K. Shahzad[7], Guillermo N. Armaiz Pena[1], Julie K. Allen[1], Rebecca L. Stone[1], Lingegowda S. Mangala[8], Hee Dong Han[1], Hye Sun Kim[1], Donna Farley[9], Gabriel Lopez Berestein[2,3,4], Steve W. Cole[5], Susan K. Lutgendorf[6], and Anil K. Sood[1,2,4]

Abstract

Purpose: Increased adrenergic activity in response to chronic stress is known to promote tumor growth by stimulating the tumor microenvironment. The focus of the current study was to determine whether dopamine, an inhibitory catecholamine, could block the effects of chronic stress on tumor growth.

Experimental Design: Expression of dopamine receptors (DR1–DR5) was analyzed by reverse transcriptase-PCR and by Western blotting. *In vitro* effects of dopamine on cell viability, apoptosis, and migration were examined. For *in vivo* therapy, murine and human DR2-siRNAs were incorporated into chitosan nanoparticles (CH-NP).

Results: In this model of chronic stress, tumoral norepinephrine levels remained elevated whereas dopamine levels were significantly decreased compared with nonstressed animals. Daily restraint stress resulted in significantly increased tumor growth in both immunodeficient (SKOV3ip1 and HeyA8) and immunocompetent (ID8) ovarian cancer models. This increase was completely blocked with daily dopamine treatment. Dopamine treatment also blocked the stress-induced increase in angiogenesis. Endothelial and ovarian cancer cells expressed all dopamine receptors except for the lack of DR3 expression in ovarian cancer cells. DR2 was responsible for the inhibitory effects of dopamine on tumor growth and microvessel density as well as the stimulatory effect on apoptosis, as the DR2 antagonist eticlopride reversed these effects. Dopamine significantly inhibited cell viability and stimulated apoptosis *in vitro*. Moreover, dopamine reduced cyclic AMP levels and inhibited norepinephrine and vascular permeability factor/VEGF-induced Src kinase activation.

Conclusions: Dopamine depletion under chronic stress conditions creates a permissive microenvironment for tumor growth that can be reversed by dopamine replacement. *Clin Cancer Res; 17(11); 3649–59.* ©2011 AACR.

Introduction

The stress response is a complex process arising from interactions between environmental contexts and the organism's evaluation of potential threat and its capacity to respond. These factors initiate a cascade of information processing in both central and peripheral nervous systems as well as hormonal cascades (1). This results in activation of the sympathetic nervous system (SNS) and the hypothalamic-pituitary-adrenal (HPA) axis (2, 3). Norepinephrine and epinephrine levels are known to be elevated in the plasma and tumor microenvironment of individuals with acute and chronic stress (4, 5). We have recently shown that both norepinephrine and epinephrine levels are elevated in a sustained fashion in ovarian and other peritoneal tissues in preclinical models of chronic stress (6). These hormonal increases were related to greater tumor burden, which was mediated by increased angiogenesis. Recent evidence suggests that the third catecholamine dopamine has the opposite effect with regard to effects on tumor angiogenesis, growth, and development of ascites (7, 8). *In vivo* and *in vitro* studies have shown that dopamine, via its specific DR2 receptors, inhibits tumor growth by suppressing the actions of vascular permeability factor (VPF)/vascular endothelial growth factor-A (VEGF-A) on both tumor endothelial cells and bone marrow–derived endothelial progenitor cells (9). Dopamine inhibits VEGF-induced angiogenesis by suppressing VEGFR-2 phosphorylation (10–12) and inhibits mitogen-activated protein kinase and focal adhesion kinase activation (12). Dopamine can also inhibit mobilization

Authors' Affiliations: Departments of [1]Gynecologic Oncology, [2]Cancer Biology, and [3]Experimental Therapeutics, and [4]Center for RNA Interference and Non-coding RNA, University of Texas MD Anderson Cancer Center, Houston, Texas; [5]Department of Medicine, Division of Hematology–Oncology, UCLA School of Medicine, Los Angeles, California; [6]Departments of Psychology and Gynecology and the Holden Comprehensive Cancer Center, University of Iowa, Iowa City, Iowa; [7]School of Medicine and Public Health, University of Wisconsin, Madison, Wisconsin; [8]Radiation Biophysics Laboratory, NASA Johnson Space Center, University of Space Research Association, Houston, Texas, and [9]Institute for Clinical and Translational Science General Hospital-Boyd Tower, Iowa City, Iowa

Note: Supplementary data for this article are available at Clinical Cancer Research Online (http://clincancerres.aacrjournals.org/).

Corresponding Author: Anil K. Sood, Department of Gynecologic Oncology, University of Texas MD Anderson Cancer Center, 1155 Herman Pressler, Unit 1362, Houston, TX 77030. Phone: (713)-745-5266; Fax: (713)-792-7586. E-mail: asood@mdanderson.org

Translational Relevance

Epidemiologic and clinical studies have provided growing evidence for links between chronic stress, depression, social isolation, and cancer progression. In the present work, our data provide a new understanding of the mechanisms by which chronic stress contributes to tumor progression. Specifically, our findings indicate that tumoral dopamine levels are depleted under chronic stress. Dopamine replacement blocked the growth stimulatory effects of chronic stress. On the basis of these findings, dopamine analogues may represent a novel therapeutic strategy.

of endothelial progenitor cells (EPC) from the bone marrow (13).

It is known that dopamine levels are increased in the brain during acute stress (14). In contrast, under chronic stress conditions, dopamine levels are lower as a consequence of decreased release of dopamine (15). However, it is not known whether dopamine levels are depleted in the tumor microenvironment in response to chronic stress. Moreover, it is not known whether dopamine can counteract the stimulatory effects of norepinephrine on tumor growth. These unanswered questions along with underlying mechanisms are addressed in this article.

Materials and Methods

Reagents

Dopamine (DA), bromocriptine [dopamine receptor 2 (DR2) agonist], eticlopride (DR2-antagonist), SKF 38393 (DR1 agonist), butaclamol (DR1 antagonist), and norepinephrine (NE) were obtained from Sigma Aldrich; recombinant human VEGF was from R&D Systems. Annexin V–(fluorescein isothiocyanate FITC) and (terminal deoxynucleotidyl transferase–mediated dUTP nick end labeling TUNEL) staining kits were purchased from BD Pharmingen and Promega, respectively.

Cell lines and culture conditions

The ovarian nontransformed (HIO-180) and cancer cells (SKOV3ip1, HeyA8, A2780, RMG2, and IGROV) were maintained in RPMI 1640, 15% FBS, and 0.1% gentamicin sulfate (16, 17). Endothelial cells isolated from the mesentery or ovary of the immortomouse (MOEC) were a kind gift from Dr. Robert Langley (18) and were maintained in DMEM, 10% FBS. All in vitro experiments were conducted at 60% to 80% confluence, unless otherwise specified. For in vivo injections, cancer cells were trypsinized and centrifuged at 1,000 rpm for 7 minutes at 4°C, washed twice, and reconstituted in Hank's balanced salt solution (Gibco).

Determination of dopamine concentration in tumor and normal tissue

Dopamine levels were determined by high-pressure liquid chromatography with electrochemical (HPLC–EC) detection in the College of Pharmacy at the University of Iowa. The method uses electrochemical detection to quantitate dopamine levels; HPLC is used to separate one catecholamine from another. Values were calculated by comparing the peak height of the unknown (sample) to that of a pure standard of known concentration, these were expressed in picograms of dopamine per milligram of wet tissue.

RT-PCR analysis of dopamine receptors

Total RNA was isolated by using the Qiagen RNeasy Kit. cDNA was synthesized by using the SuperScript First-Strand Kit (Invitrogen) as per the manufacturer's instructions. cDNA was subjected to PCR using specific primer sequences for human dopamine receptors (DR1–DR5) previously reported (19). Specific primer sequences for murine dopamine receptors (DR1–DR5) were designed on the basis of the reported NCBI nucleotide sequences using the Oligo Perfect Software (Invitrogen). β-Actin was used as a housekeeping gene.

siRNA preparation

Specific siRNA sequences targeted against murine dopamine receptor 2 (DR2; duplex of 5′-GAUUCACUGUGACAUCUUU and 5-AAAGAUGUCACAGUGAAUC) and human DR2 (duplex of 5′-CACACAUCCUGAACAUCA and 5′-UGUAUGUUCAGGAUGUGUG) were obtained from Sigma Aldrich. These sequences were incorporated into chitosan nanoparticles (CH-NP) by using a gelation method of anionic tripolyphosphate (TPP; ref. 20). Briefly, predetermined TPP (0.25% w/v) and siRNA (1 μg/μL) were added in CH solution, resulting in siRNA-CH-NP generated under constant stirring at room temperature. After incubating at 4°C for 40 minutes, the siRNA-CH was collected by centrifugation (Thermo Biofuge) at 12,000 rpm for 40 minutes at 4°C. The CH-NPs were purified 3 times and stored at 4°C until used.

Chronic stress model and treatment schema

Female athymic nude and immunocompetent (C57BL6) mice (10- to 12-week-old) were obtained from the U.S. National Cancer Institute. All experiments were approved by the Institutional Animal Care and Use Committee of the University of Texas MD Anderson Cancer Center. The animals were experimentally stressed using a well-characterized restraint system, in which periodic immobilization induces high levels of HPA and SNS activity characteristic of chronic stress (6). Ovarian cancer cells were injected intraperitoneally into mice 7 days after starting daily stress applied for 2 hours. Then, mice were further divided into treatment groups (10 animals per group) as follows: (i) control PBS, (ii) dopamine [75 mg/kg daily intraperitoneal (i.p.)], (iii) dopamine + eticlopride (10 mg/kg daily i.p); (iv) control siRNA-CH; (v) dopamine + murine dopamine receptor 2-siRNA (mDR2-siRNA-CH (5 μg per injection); or (vi) dopamine + human dopamine receptor 2-siRNA (hDRD2-siRNA; 5 μg per injection). siRNA treatments (150 μg/kg) were

given through the i.v. route twice per week. Following 3 weeks of treatment, mice were euthanized and tumor weight and nodules were recorded. Tumor and relevant tissue samples were collected.

Cell viability assay

To examine the effect of dopamine on cell viability, MTT assay was carried out as previously described (21).

Cyclic AMP determination

The effect of dopamine on cyclic AMP (cAMP) accumulation was examined exposing cells to 0, 10, and 50 µmol/L dopamine for 30 minutes at 37°C. cAMP levels were measured in total cell lysates using an enzyme immunoassay kit (Biomol).

Cell invasion assay

Invasion through human-defined matrix was assessed using the Membrane Invasion Culture System (MICS), as previously described (22). A total of 1.5×10^5 SKOV3ip1 cells were loaded into the upper chamber in media only or in media containing the stimulant of interest. Agonist (DR1, SKF 38393; DR2, bromocriptine) and antagonist (DR1, butaclamol; DR2, eticlopride) were used at 50 µmol/L, norepinephrine at 10 µmol/L, and VEGF at 10 ng/mL. Cells were allowed to invade in a humidified incubator for 24 hours. Cells that had invaded through the basement membrane were collected, stained, and counted by light microscopy in 5 random fields (original magnification × 200) per sample.

Western blot and immunoprecipitation analyses

Western blot analysis was carried out as previously described (21). Briefly, lysates from cultured cells were prepared using modified radioimmunoprecipitation assay (RIPA) buffer, protein concentrations were determined using a BCA Protein Assay Reagent kit (Pierce Biotechnology). Protein lysates were subjected to 10% SDS–PAGE separation and transferred to a nitrocellulose membrane. Blots were probed with primary antibodies DR2 (Santa Cruz Biotechnology), Src and phosphorylated Src^{Y416} (pSrc^{Y416}) kinase (Cell Signaling Biotechnology), and horseradish peroxidase–conjugated secondary antibody (Amersham) and developed with enhanced chemiluminescence detection kit (ECL; Pierce Biotechnology). Equal protein loading was confirmed reprobing membranes with an anti-β-actin antibody (Sigma Aldrich). To examine the association between Gαi1-protein and DR2, MOEC cells were exposed to 10 µmol/L dopamine for 0, 10, and 30 minutes at 37°C. Cell lysates were than prepared and immunoprecipitated with DR2 antibody at 4°C for 2 hours. Immunocomplexes were captured with 2% protein A–agarose beads (Upstate). Protein was eluted in reducing sample Laemmli buffer, subjected to 10% SDS–PAGE separation, and transferred to a nitrocellulose membrane. Anti-Gαi (Abcam) was used as primary antibody. Immunodetection of Gαi1-protein was carried out as described earlier.

Immunohistochemistry

Analysis of microvessel density (MVD) and assessment of tumor and endothelial cell apoptosis were conducted following procedures described previously (18, 21, 23, 24). Double immunofluorescence for DR2/CD31 and for DR2/TUNEL was carried out in frozen tissue sections as follows: after acetone fixation and blocking with gelatin (4%), tissues were incubated with rabbit DR2 antibody (Santa Cruz Biotechnology; 1:100) at 4°C overnight. Samples were washed in PBS and incubated with blocking solution for 10 minutes and then with a goat anti-rabbit Alexa 488 antibody (1:1,000) for 1 hour. Afterward, tissues were subjected to CD31 and TUNEL staining, as previously described. (18, 21, 23, 24).

Immunofluorescence and confocal microscopy

Immunofluorescence microscopy was carried out using a Zeiss Axioplan fluorescence microscope (Carl Zeiss, Inc.) equipped with a 100-W Hg lamp and narrow band-pass excitation filters. Representative images were obtained using a cooled charge-coupled device Hamamatsu C5810 camera (Hamamatsu Photonics) and Optimas software (Media Cybernetics). Confocal fluorescence images were collected using 20× objectives on a Zeiss LSM 510 laser scanning microscopy system (Carl Zeiss, Inc.) equipped with a motorized Axioplan microscope, argon laser (458/477/488/514 nm, 30 mW), HeNe laser (413 nm, 1 mW, and 633 nm, 5 mW), LSM 510 control and image acquisition software, and appropriate filters (ChromaTechnology Corp.). Composite images were constructed with Photoshop software (Adobe Systems, Inc.).

In vitro assessment of apoptosis

MOEC and SKOV3ip1 cells were exposed to different dopamine concentrations (0–50 µmol/L) for 48 hours. The relative percentage of apoptotic cells was assessed using the Annexin V-FITC Apoptosis Detection Kit-1 (BD Pharmingen) according to the manufacturer's protocol.

Statistical analysis

Continuous variables were compared with the Student t test (between 2 groups) or analysis of variance (for all groups) if normally distributed and the Mann–Whitney rank-sum test if distributions were nonparametric. For *in vivo* therapy experiments, 10 mice in each group were used, and a $P < 0.05$ on 2-tailed testing was considered significant. To control for the effects of multiple comparisons, a Bonferroni adjustment was made; for the analysis, a value of $P \leq 0.017$ was considered statistically significant.

Results

Dopamine levels during chronic stress

We determined dopamine and norepinephrine concentrations in tumors and peritoneal tissues including ovary, liver, and omentum from mice subjected to daily stress for 1, 3, 7, or 14 days. Norepinephrine levels increased after 1 day of stress and remained elevated until day 14 in all

tissues samples. In contrast, dopamine concentrations increased significantly after 1 day of stress but declined after 3 to 14 days of stress in tumor, ovarian, and omental tissues (Supplementary Fig. S1).

Dopamine dose–response *in vivo*

We have previously shown that chronic stress establishes favorable conditions for promoting angiogenesis in the tumor microenvironment by SNS activation (6). Because the levels of dopamine, the antiangiogenic catecholamine, are decreased in the tumor microenvironment under chronic stress, we asked whether dopamine could block the stimulatory effects of SNS on ovarian cancer growth. Before conducting such blocking experiments, we first tested several doses of dopamine to identify the lowest dose required for inhibiting cancer growth in nonstressed or stressed mice. SKOV3ip1 tumor–bearing nude mice ($n = 10$ per group) were treated with (i) control PBS, (ii) dopamine at 50 mg/kg, (iii) dopamine at 75 mg/kg, or (iv) dopamine at 100 mg/kg. Treatment was started 1 week after injection of SKOV3ip1 ovarian cancer cells. In stressed mice, doses of 75 and 100 mg/kg significantly reduced tumor growth ($P < 0.05$), with the greatest decrease noted at the 75 mg/kg dose. All 3 doses significantly decreased the number of tumor nodules ($P < 0.05$) compared with controls (Supplementary Fig. S2A). In contrast, in nonstressed mice, no significant changes in tumor weight or tumor nodules were observed at any of the dopamine doses tested. Given the known effects of dopamine on angiogenesis (7), we also assessed MVD. There was a significant reduction in MVD at all dopamine doses tested ($P < 0.05$; Supplementary Fig. S2B). Dopamine at 75 mg/kg was selected for all subsequent *in vivo* experiments because of its inhibitory effect on cancer growth.

To assess the longitudinal effects of dopamine, we carried out an *in vivo* experiment in SKOV3ip1 tumor–bearing mice. Tumor growth curves in nonstressed and stressed mice are presented in Supplementary Figure S2D. Although there was no significant effect of dopamine in the nonstress setting, dopamine completely blocked the growth stimulatory effects of daily restraint stress (Supplementary Fig. S2D).

Dopamine blocks stress-induced ovarian cancer growth via DR2

As expected, daily stress increased tumor growth by 2.4-fold (Fig. 1). In stressed mice, daily dopamine treatments resulted in 68% reduction in tumor growth compared with control mice injected with PBS ($P < 0.05$). We also tested the effects of dopamine in an immunocompetent syngeneic mouse model of ovarian cancer (ID8-C57BL6 model). Consistent with the other models, daily restraint stress increased tumor growth by 50% ($P < 0.01$; Supplementary Fig. S3) in the ID8 model. Moreover, dopamine treatment significantly reduced tumor growth (47%; $P < 0.02$) in the nonstressed group and blocked the stress-mediated increase in tumor growth (78%, $P < 0.001$; Supplementary Fig. S3).

Because dopamine can signal through multiple receptors, we examined the RNA expression of DR1–DR5 in ovarian and endothelial cell lines. Figure 1A shows the RNA expression in ovarian nontransformed epithelial (HIO-180), cancer (A2780, HeyA8, and SKOV3ip1), and endothelial cells [human umbilical vein endothelial cells (HUVEC)]. Although all dopamine receptors are expressed in HUVEC, DR3 was not detected in any of the ovarian cell lines tested. Protein expression of DR1 and DR2 was also confirmed by Western blotting in these and other ovarian cancer cell lines (RMG2 and IGROV) as well as MOEC cells (Fig. 1A).

Given the probable role of DR2 in mediating the antiangiogenic effects of dopamine (7), we next examined whether the suppression of tumor growth by dopamine was specifically mediated by DR2. In stressed mice, the addition of a DR2 antagonist (eticlopride) to dopamine treatment reversed the protective effects of dopamine (Fig. 1B). These data suggest that dopamine indeed acted through DR2 to block stress-mediated ovarian cancer growth.

Dopamine targets murine endothelial and human cancer cells

To further examine whether the inhibitory effects of dopamine were mediated by targeting (host) endothelial and/or (human) tumor cells through their corresponding DR2 receptors, we utilized siRNA incorporated into CH-NPs. The specificity of siRNA sequences for mouse and human DR2 was confirmed using RT-PCR (Supplementary Fig. S4). SKOV3ip1 tumor–bearing mice were divided into 4 experimental groups: (i) control siRNA, (ii) dopamine alone, (iii) dopamine + mDR2-siRNA, and (iv) dopamine + hDR2-siRNA; each group was used for both nonstress and stress conditions (Fig. 1C). In daily stressed mice, dopamine treatment significantly blocked tumor weight (67%) and the number of tumor nodules (65%). This growth inhibitory effect of dopamine was significantly abrogated by dopamine/mDR2-siRNA-CH but not by dopamine/hDR2-siRNA-CH combined treatment ($P = 0.02$; Fig. 1C). These results suggest that in the SKOV3ip1 model, dopamine-mediated effects occur primarily through DR2 on endothelial cells. The effects of dopamine were also tested in a second ovarian cancer model, HeyA8 (Fig. 1D). Compared with mice injected with control siRNA, dopamine treatment blocked tumor growth by 84% ($P = 0.007$) and resulted in a 63% decrease in the number of nodules ($P = 0.02$). Interestingly, in this model, both dopamine/mDR2-siRNA-CH and dopamine/hDR2-siRNA-CH treatments significantly blocked the inhibitory effects of dopamine.

Effect of dopamine on angiogenesis and cell viability

Given the known effects of catecholamines on angiogenesis, we examined MVD in the SKOV3ip1 tumors harvested from dopamine-treated animals. In stressed mice, dopamine treatment resulted in a significant reduction (61%) in MVD compared with controls (Fig. 2A; $P < 0.01$). In
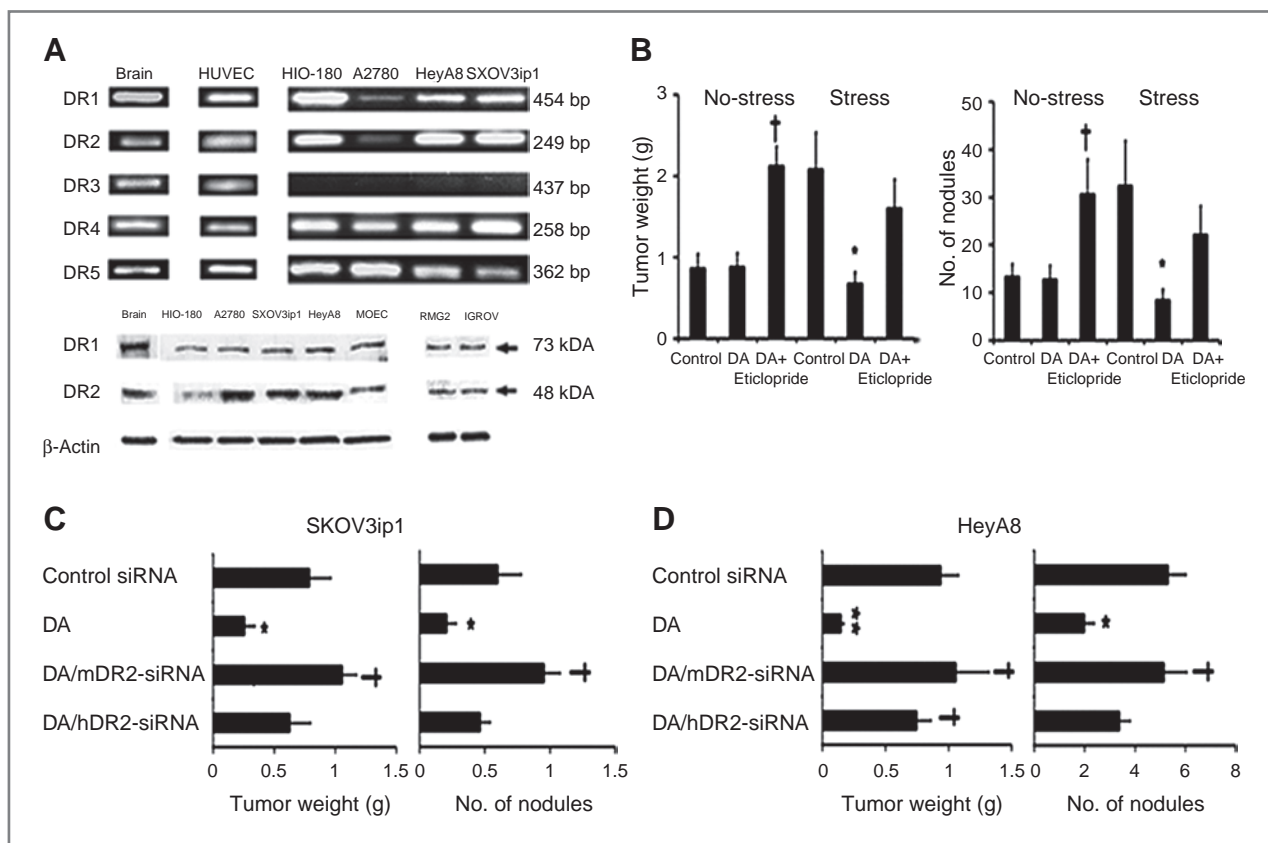
Figure 1. Dopamine (DA) blocks stress-mediated tumor growth by acting through DR2. A, RT-PCR analysis of DR1–DR5 and protein expression of DR1–DR2 in endothelial and ovarian cancer cell lines. HUVECs and MOEC cells express all 5 receptors, whereas DR3 was not detected in ovarian cancer cells. B, tumor weight and tumor nodules in nonstressed and stressed mice bearing SKOV3ip1 tumors treated with: PBS (control), DA, and DA/eticlopride. DA blocked significantly tumor growth and reduced number of tumor nodules in stressed mice. This effect was abrogated by the combined treatment of DA/eticlopride. In nonstressed mice DA/eticlopride treatment significantly increased tumor growth compared with controls. Data are the mean $\pm$ SE; $n = 10$ mice per group. *, $P < 0.05$ compared with stress controls, †, $P < 0.005$ compared with nonstress controls. C and D, tumor weight and tumor nodules in stressed mice bearing SKOV3ip1 and HeyA8 tumors treated with control siRNA, DA, DA/mDR2-siRNA-CH, and DA/hDR2-siRNA-CH. DA reduced significantly tumor growth and tumor nodules in the SKOV3 ip1 ($P < 0.05$) and HeyA8 models ($P < 0.01$). The combined treatment of DA/mDR2-siRNA significantly abrogated the DA inhibitory effect on tumor growth in the SKOV3ip1 model. In the HeyA8 model, both combined treatments (DA/mDR2-siRNA-CH and DA/hDR2) reversed the DA-blocking effect on tumor growth. Data are the mean $\pm$ SE; $n = 10$ mice per group. *, $P < 0.05$; **, $P < 0.01$, compared with controls; †, $P < 0.05$, compared with DA-treated mice.

contrast, dopamine/eticlopride treatment led to a significant increase (Fig. 2A; $P < 0.01$) in MVD compared with dopamine-treated mice. We also examined effects on tumor cell apoptosis, as it is known that norepinephrine can reduce sensitivity of cancer cells to apoptosis (19). Tissues from dopamine-treated mice revealed a 2.2-fold increase ($P < 0.01$) in tumor cell apoptosis compared with control tissues (Fig. 2A). The combined dopamine/eticlopride treatment abrogated the dopamine-mediated effects on cell apoptosis. In addition, the combined treatment of dopamine/mDR2-siRNA and dopamine/hDR2-siRNA-CH reversed the effects of dopamine on MVD ($P < 0.01$) and cell apoptosis ($P < 0.01$; Fig. 2B). Colocalization of DR2 in tumor cells and tumor-associated endothelial cells was confirmed by double immunofluorescence staining for CD31 antigen/DR2 and TUNEL/DR2. Confocal images are included in Figure 2A and B.

To determine whether the effects of dopamine on tumor growth are direct or indirect, we carried out a series of in vitro experiments. First, effects of dopamine on in vitro viability of ovarian cancer or endothelial cells were tested. Dopamine did not significantly affect viability of the nontransformed (HIO-180) or ovarian cancer cells (A2780 and SKOV3ip1; Fig. 3). However, cell viability of HeyA8 ovarian cancer cells was significantly decreased at dopamine doses from 12.5 to 50 μmol/L. This is consistent with the in vivo inhibitory effect of dopamine on HeyA8 tumor growth. In MOEC cells, there was a dose-dependent decrease in cell viability with increasing doses of dopamine ($P < 0.01$; Fig. 3).

We also examined the effects of dopamine on apoptosis in MOEC and SKOV3ip1 cells after treatment for 48 hours. The percentage of early apoptosis increased proportionally to dopamine concentrations used in MOEC (Fig. 3),
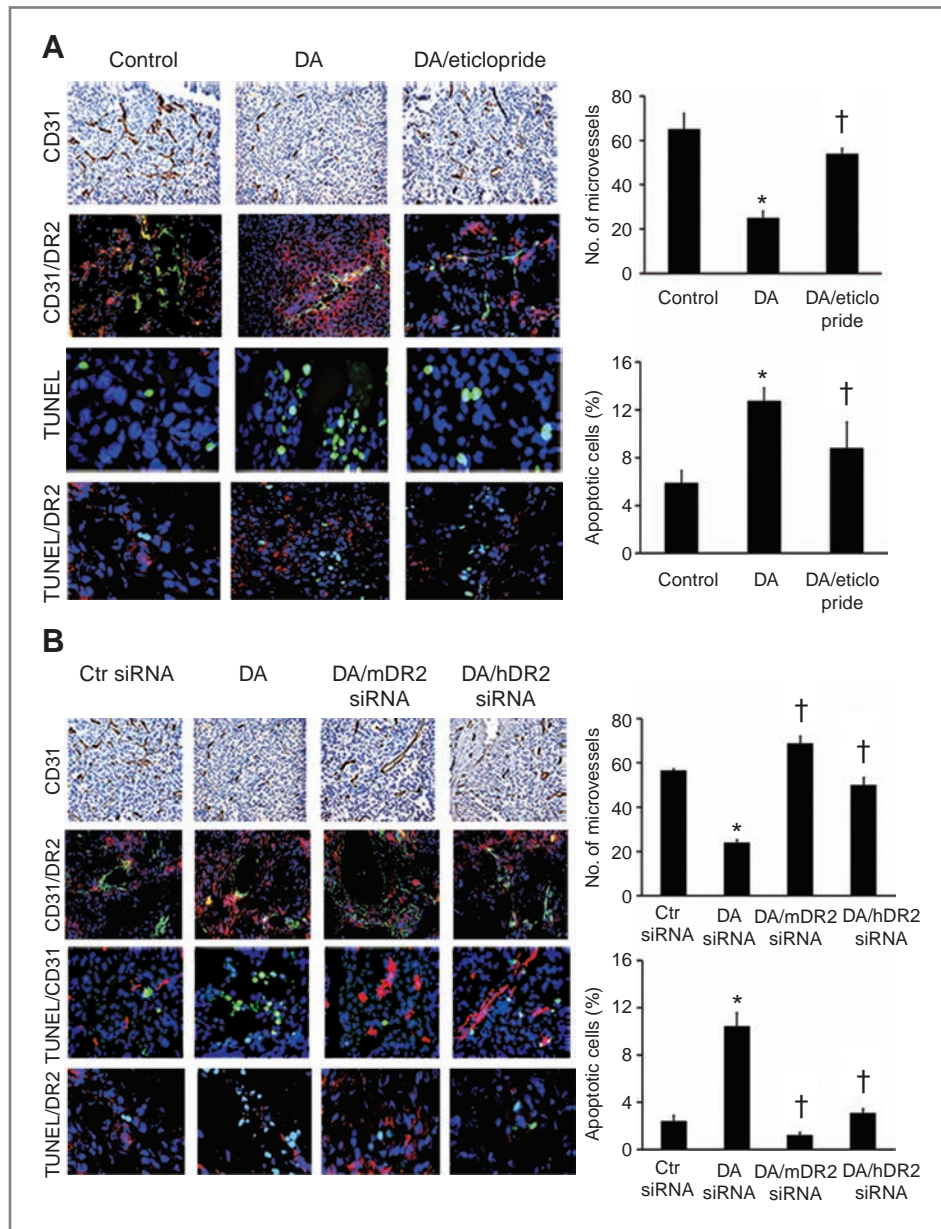
Figure 2. Dopamine (DA) decreases stress-stimulated angiogenesis and stimulates tumor cell apoptosis via its DR2. A, MVD was significantly decreased by DA treatment in SKOV3ip1 tumor tissues of stressed mice (*, $P < 0.01$). DA/eticlopride treatment significantly (†, $P < 0.01$) reversed DA inhibitory effect on MVD, which was evaluated by immunohistochemical analysis of CD31 [3,3′-diaminobenzidine (DAB) staining]. Microvessels were counted in 5 fields at 100× of each tissue sample ($n = 5$). Values are means ± SE. DA treatment caused significantly (*, $P < 0.005$) higher apoptotic rates than control mice. This effect was also significantly (†, $P < 0.005$) reversed by DA/eticlopride combined treatment. Confocal images (200×) showing colocalization of DR2 (red fluorescence) in CD31-positive tumor endothelial cells (green fluorescence). Apoptotic cells (green fluorescence) were detected by TUNEL staining (Promega kit). Percentages of apoptotic cells were calculated in 5 fields at 200× of each tissue sample ($n = 5$). Values are mean ± SE. Detection of DR2 (red fluorescence) in tumor apoptotic cells (green fluorescence). Confocal images 200×. B, DA/mDR2-siRNA and DA/hDR2-siRNA-CH combined treatments induced significant increase (†, $P < 0.005$) in MVD in stressed mice, reverting the DA inhibitory effect on MVD (*, $P < 0.005$). Values are mean ± SE. Detection of DR2 (red fluorescence) in tumor CD31-positive endothelial cells (green fluorescence). Confocal images 200×. DA stimulatory effect on tumor cell apoptosis was also significantly abrogated by the DA/mDR2-siRNA and DA/hDR2-siRNA treatments (†, $P < 0.005$). Values are mean ± SE. Confocal images (200×) revealing colocalization of DR2 (red fluorescence) in tumor apoptotic cells (green fluorescence).

whereas late apoptotic rates did not vary. Total apoptotic rates in these cells were significantly elevated at 25 μmol/L (51%) and 50 μmol/L (75%) compared with untreated cells ($P < 0.01$). SKOV3ip1 cells showed significantly higher percentages of late apoptotic cells at 50 μmol/L dopamine ($P < 0.01$).
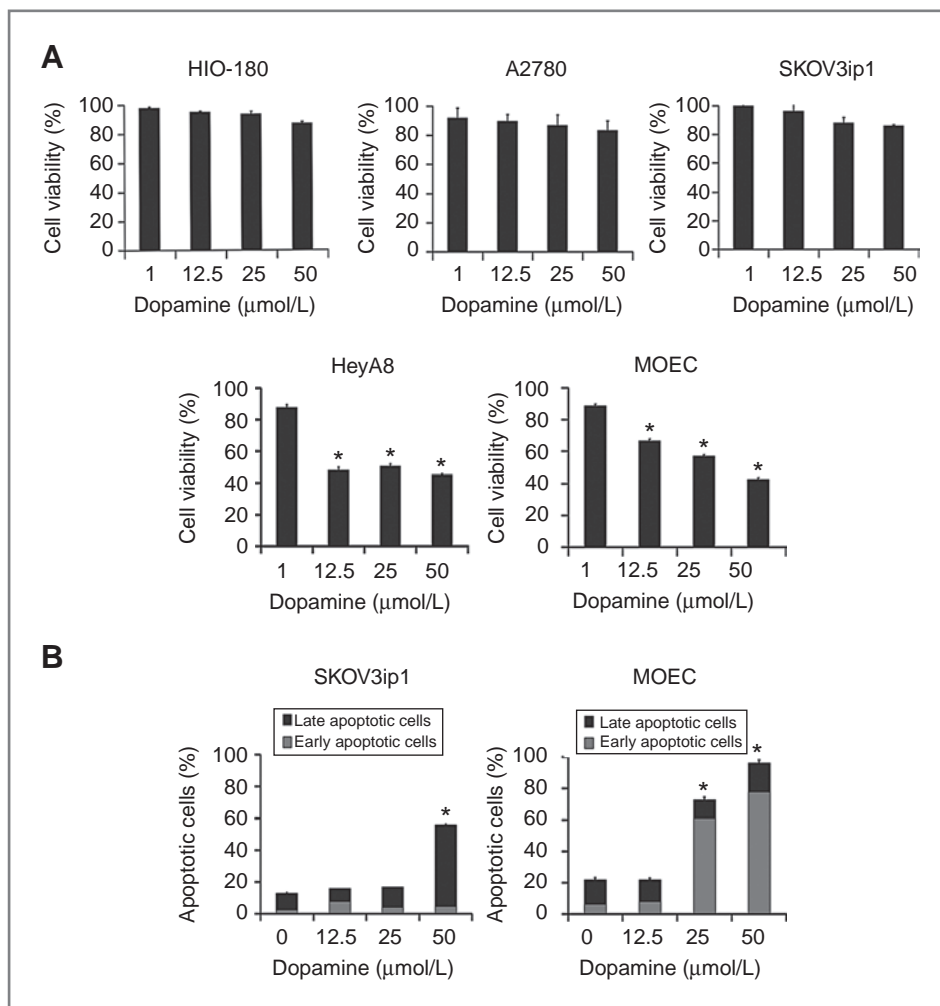
Figure 3. Effect of dopamine (DA) on cell viability and *in vitro* cell apoptosis. A, DA (12.5–50 µmol/L) significantly reduced cell viability of HeyA8 ovarian cancer cells (*, $P < 0.005$) and caused a dose-dependent decrease in MOEC cell viability (*, $P < 0.01$). B, apoptotic rates were significantly increased by DA exposure (25 and 50 µmol/L) in MOEC cells and at 50 µmol/L DA in SKOV3 ip1 cells. Values are means ± SE of 3 independent experiments.

Dopamine counteracts the stimulatory effect of VEGF and norepinephrine on tumor cell invasion

Although dopamine did not affect cell viability of all ovarian cancer cells tested, we explored whether it could affect other steps in the metastatic cascade. We examined the effects of dopamine on cell invasion. We analyzed the effect of dopamine and various dopamine agonists and antagonists on the invasive potential of SKVO3ip1 cells. Dopamine at 10 µmol/L inhibited VPF/VEGF-induced cell invasion (25) by 59% ($P < 0.05$; Fig. 4), as did the DR2 agonist bromocriptine (56%; $P < 0.05$). However, the DR1 agonist SKF 38393 (50 µmol/L) had no effect. Eticlopride (50 µmol/L), a specific DR2 receptor antagonist, significantly abrogated the dopamine-mediated inhibition of cancer cell invasion ($P < 0.01$). These results further suggest that the inhibitory action of dopamine on cell invasion was mediated specifically through DR2.

We also examined whether dopamine can block the stimulatory effect of norepinephrine on SKOV3ip1 cell invasion, previously described by our group (22). Dopa-

mine blocked the norepinephrine-mediated effect by 61% ($P < 0.05$) in SKOV3ip1 cells exposed to norepinephrine plus dopamine. In addition, the combined treatment of dopamine/norepinephrine/VEGF led to a 52% reduction ($P < 0.001$) in cell invasion compared with norepinephrine/VEGF treatment, indicating the ability of dopamine to counteract the stimulatory effects of norepinephrine and VEGF on cell invasion (Fig. 4).

Dopamine decreases cAMP levels in MOEC and SKOV3ip1 cells

Dopamine, acting through G-protein–coupled receptors, exerts stimulatory (DR1, DR5) or inhibitory (DR2–DR4) effects on adenylate cyclase leading to increased and decreased intracellular cAMP levels, respectively. We examined the effects of dopamine on cAMP levels in MOEC and SKOV3ip1 cells. Dopamine at 10 µmol/L resulted in a reduction in intracellular cAMP levels by 31% and 70% in MOEC and SKOV3ip1 cells, respectively (Fig. 5A). Further decreases in cAMP levels were noted at higher doses (50 µmol/L) of dopamine.
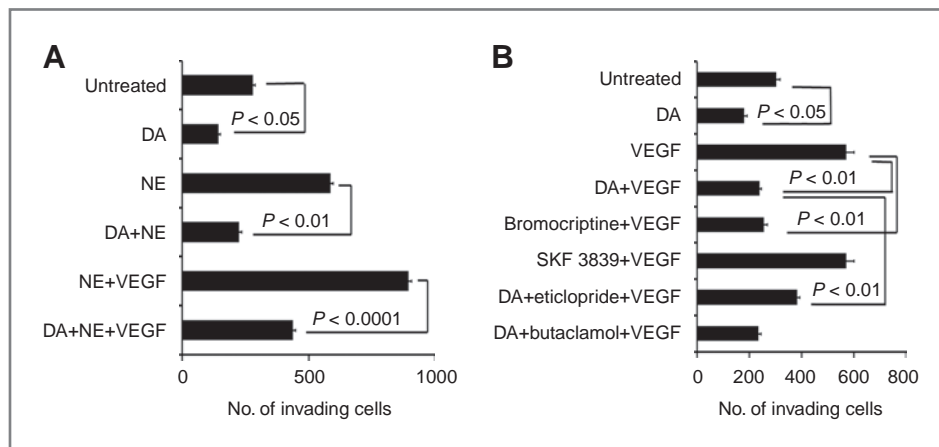
Figure 4. Effect of dopamine (DA) and various DA agonists and antagonists on VPF/VEGF- and norepinephrine (NE)-stimulated SKOV3ip1 cell invasion. A, DA and the DR2 agonist (bromocriptine) significantly inhibited the VPF/VEGF-induced cell invasion ($P < 0.05$); eticlopride, a DR2-specific antagonist, abrogated the DA-mediated inhibition of VPF/VEGF-induced cell invasion, whereas butaclamol, a DR1-specific antagonist, did not affect cell invasion. B, DA blocked the stimulatory effect of NE alone ($P < 0.05$) and NE+ VEGF ($P < 0.001$) on cell invasion. Values are means ± SE of 3 independent experiments.

Dopamine inhibits VEGF- and norepinephrine-induced cell signaling

The effect of dopamine on phosphorylation of several key effectors of the VEGF angiogenic pathway was analyzed in MOEC and SKOV3ip1 cells. In MOEC cells, VEGF (10 ng/mL) for 15 minutes resulted in increased phosphorylation of Src^{Y416} (Fig. 5B). This effect was blocked by a 10-minute preincubation of cells with dopamine at 10 μmol/L. Similarly, SKOV3ip1 cells stimulated with norepinephrine (10 μmol/L) for 5 minutes revealed a significant increase (2.4-fold) of $pSrc^{Y419}$ (Fig. 5B), which was blocked by a combined treatment of dopamine + norepinephrine for 5 and 15 minutes.

Our *in vitro* data confirmed that dopamine decreases intracellular cAMP levels in MOEC and SKOV3ip1 cells. This strongly suggested that dopamine could be acting through the DR2–cAMP signaling pathway to exert its inhibitory effects *in vivo* on tumor growth. To address this question, we examined the association of DR2 to Gαi1-protein in MOEC cells exposed to dopamine (10 μmol/L) for 10 and 30 minutes. There was a 1.6-fold increase in the interaction between DR2 and Gαi1-protein after 10 minutes of dopamine exposure compared with untreated cells (Fig. 5C).

Discussion

The main findings of this study are that dopamine significantly reduces stress-mediated cancer growth in ovarian carcinoma. Our data strongly suggest that dopamine retards tumor growth by inhibiting tumor angiogenesis and stimulating tumor cell apoptosis. In addition, we provide the first evidence that dopamine can block the stimulatory effects of chronic stress on cancer growth.

The physiologic actions of dopamine are mediated by at least 5 distinct G-protein–coupled receptor subtypes. (26, 27). Two DR1-like receptor subtypes (DR1 and DR5) couple to the G-protein Gs, activate adenylate cyclase, and increase cAMP levels. The other receptor subtypes belong to the DR2-like subfamily (DR2, DR3, and DR4) and are prototypic of G-protein–coupled receptors that inhibit adenylate cyclase and decrease cAMP production. The ovarian nontransformed cancer and endothelial cells tested in this work showed expression of DR1- and DR2-like dopamine receptors, indicating that dopamine might regulate stimulatory and/or inhibitory processes in these cells.

Dysfunction of dopaminergic system is known to be associated with various disorders, including schizophrenia and Parkinson's disease (28). The consequences of dopamine dysfunction indicate the importance of maintaining dopamine functionality through homeostatic mechanisms based on the delicate balance between synthesis, storage, release, metabolism, and reuptake (28). A decrease in dopamine in the brain has been implicated as the cause of Parkinson's disease. In contrast, it is argued that a functional excess of dopamine or oversensitivity of certain DRs is one of the causal factors in schizophrenia (29). Interestingly, the incidence of cancer in patients with schizophrenia has been reported to be lower than in the general population (30–32). Whether this reduced incidence is related to hyperactive dopaminergic system is not known.

It has been shown that dopamine concentrations are lower in the tumor microenvironment than in normal tissues (11, 33). These findings prompted us to consider whether the increases in tumor growth and angiogenesis may result from a permissive microenvironment created by a relative shift toward growth-promoting catecholamines. In the present study, we show that dopamine blocks stress-induced tumor growth by activating DR2. The central role of DR2 was confirmed with the DR2 antagonist eticlopride in combination therapy with dopamine, as well as with siRNA targeted against murine or

Figure 5. Dopamine (DA) decreases intracellular cAMP levels and inhibits VPF/VEGF- and norepinephrine (NE)-stimulated Src activation. A, DA at 10 and 50 μmol/L caused a significant decrease of intracellular cAMP levels in MOEC and SKOV3ip1 cells. Values are means ± SE of 3 independent experiments; *, $P < 0.001$ for MOEC cells; *, $P < 0.05$ for SKOV3 ip1 cells. B, in MOEC cells, preincubation with DA at 10 μmol/L for 10 minutes inhibited the VPF/VEGF-stimulated phosphorylation of Src^{Y416}. In SKOV3 ip1 cells, DA reverted the stimulatory effect of NE on Src^{Y419} phosphorylation by combined treatment of NE+ DA for 5 and 15 minutes. Phospho-Src densitometric data were normalized to total Src; these are representative of 2 independent experiments. C, DA induces association of DR2 to Gαi-protein. MOEC cells were exposed to 10 μmol/L DA for 10 and 30 minutes. MOEC lysates were then immunoprecipitated with DR2 antibody and analyzed by Western blotting. Gαi-protein was immunodetected using a specific anti-Gαi antibody (Abcam). DA caused a 1.6-fold higher interaction between DR2 and Gαi-protein after 10 minutes of exposure compared with untreated cells. The densitometric data were normalized to a loading control (β-actin from original lysate) and are representative of 2 independent experiments. IP, immunoprecipitation.
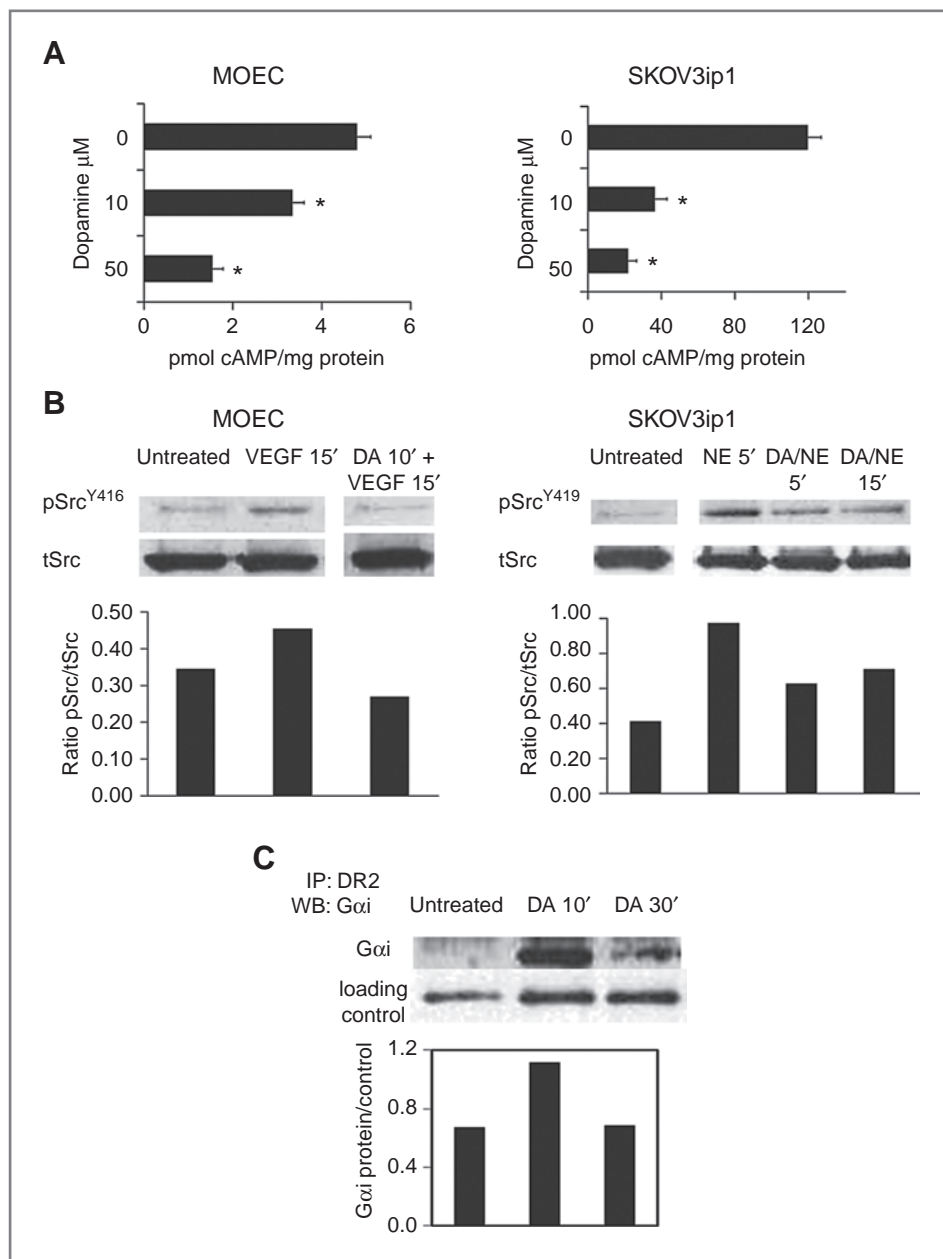
human DR2. The dopamine-suppressing effect on tumor growth in our stress models was significantly blunted by *DR2* gene silencing. These findings indicate that dopamine targets both host murine endothelial cells and human cancer cells through DR2 to exert its growth-suppressive effects. Our results are supported by the reported growth inhibitory effects of dopamine under nonstress conditions (7, 9, 34).

Our data also indicate that dopamine, via DR2, blocked the VPF/VEGF or norepinephrine-mediated invasion of ovarian cancer cells. The inhibitory effects of dopamine on cell invasion would explain, in part, the *in vivo* blocking effect of dopamine on tumor progression and metastasis

under chronic stress. Our *in vitro* studies show that dopamine decreases viability not only of endothelial cells, as previously described (7, 12) but also of ovarian cancer cells. These results were further confirmed using *in vivo* models of ovarian carcinoma. The dual cell targeting (endothelial and tumor cells) of dopamine in the tumor microenvironment underlines the significance of dopamine as a potential modality to block the growth stimulatory effects of chronic stress.

Dopamine and DR2 agonists have been used for many years for the treatment of Parkinson's disease and hyperprolactinemia (35, 36) as well as for the management of cardiovascular disorders and renal dysfunction. (37, 38).

Dopamine agonists such as bromocriptine mesylate (Parlodel, oral) have also been used clinically to treat hyperprolactinemia and are well tolerated (39). Furthermore, effective shrinkage of prolactinomas has been observed after injection of long-acting form of Parlodel (40). Such agents may represent a new strategy for blocking the effects of chronic stress on tumor growth. With such therapies, however, some adverse reactions such as nausea, hallucinations, and orthostatic hypotension have been reported and would require careful monitoring.

To identify the signaling pathways by which dopamine affects endothelial and ovarian cancer cell function, we examined the effects of dopamine on phophorylation and activation of various effectors in the metastatic cascade. In MOEC cells, dopamine inhibited VEGF-induced phophorylation and activaton of Src kinase. In addition, dopamine reversed norepinephrine-stimulated Src phosphorylation. Src is a key mediator in multiple signaling pathways that regulate critical cellular functions (41). In ovarian cancer, Src has been shown to play a functional role in cancer cell invasion and angiogenesis (42). Src is also a regulator of VEGF-mediated vascular permeability (43). Recent studies in HUVECs have shown that dopamine reduces VEGF-mediated permeability by inhibiting VEGF-induced Src activation (44). These studies coupled with our data implicate blockade of Src activation as a key mediator of the inhibitory effects of dopamine on ovarian cancer growth.

Overall, our data suggest that dopamine inhibits stress hormone–stimulated Src activation in endothelial and ovarian cancer cells. Moreover, we conclude that dopamine replacement effectively counteracts the stimulatory effects of norepinephrine on ovarian cancer growth during chronic stress. Considering the stimulatory effects of chronic stress on cancer growth (6), our findings implicate dopamine as a potential therapeutic strategy for blocking the deleterious effects of chronic stress.

Disclosure of Potential Conflicts of Interest

No potential conflicts of interest were disclosed.

Grant Support

References

1. Weiner H. Perturbing the Organism: The Biology of Stressful Experience. Chicago, IL: University of Chicago Press; 1992.
2. Glaser R, Kiecolt-Glaser JK. Stress-induced immune dysfunction: implications for health. Nat Rev Immunol 2005;5:243–51.
3. Antoni MH, Lutgendorf SK, Cole SW, Dhabhar FS, Sephton SE, McDonald PG, et al. The influence of bio-behavioural factors on tumour biology: pathways and mechanisms. Nat Rev Cancer 2006;6:240–8.
4. Schmidt C, Kraft K. Beta-endorphin and catecholamine concentrations during chronic and acute stress in intensive care patients. Eur J Med Res 1996;1:528–32.
5. Lutgendorf SK. Depression, social support, and beta-adrenergic transcription control in human ovarian cancer. Brain Behav Immun 2009;23:176–83.
6. Thaker PH, Han LY, Kamat AA, Arevalo JM, Takahashi R, Lu C, et al. Chronic stress promotes tumor growth and angiogenesis in a mouse model of ovarian carcinoma. Nat Med 2006;12:939–44.
7. Basu S, Nagy JA, Pal S, Vasile E, Eckelhoefer IA, Bliss VS, et al. The neurotransmitter dopamine inhibits angiogenesis induced by vascular permeability factor/vascular endothelial growth factor. Nat Med 2001;7:569–74.
8. Teunis MA, Kavelaars A, Voest E, Bakker JM, Ellenbroek BA, Cools AR, et al. Reduced tumor growth, experimental metastasis formation, and angiogenesis in rats with a hyperreactive dopaminergic system. FASEB J 2002;16:1465–7.
9. Chakroborty D, Sarkar C, Basu B, Dasgupta PS, Basu S. Catecholamines regulate tumor angiogenesis. Cancer Res 2009;69:3727–30.
10. Basu S, Sarkar C, Chakroborty D, Nagy J, Mitra RB, Dasgupta PS, et al. Ablation of peripheral dopaminergic nerves stimulates malignant tumor growth by inducing vascular permeability factor/vascular endothelial growth factor-mediated angiogenesis. Cancer Res 2004;64:5551–5.
11. Chakroborty D, Sarkar C, Mitra RB, Banerjee S, Dasgupta PS, Basu S. Depleted dopamine in gastric cancer tissues: dopamine treatment retards growth of gastric cancer by inhibiting angiogenesis. Clin Cancer Res 2004;10:4349–56.
12. Sarkar C, Chakroborty D, Chowdhury UR, Dasgupta PS, Basu S. Dopamine increases the efficacy of anticancer drugs in breast and colon cancer preclinical models. Clin Cancer Res 2008;14:2502–10.
13. Chakroborty D, Chowdhury UR, Sarkar C, Baral R, Dasgupta PS, Basu S. Dopamine regulates endothelial progenitor cell mobilization from mouse bone marrow in tumor vascularization. J Clin Invest 2008;118:1380–9.
14. Puglisi-Allegra S, Imperato A, Angelucci L, Cabib S. Acute stress induces time-dependent responses in dopamine mesolimbic system. Brain Res 1991;554:217–22.
15. Imperato A, Angelucci L, Casolini P, Zocchi A, Puglisi-Allegra S. Repeated stressful experiences differently affect limbic dopamine release during and following stress. Brain Res 1992;577:194–9.
16. Buick RN, Pullano R, Trent JM. Comparative properties of five human ovarian adenocarcinoma cell lines. Cancer Res 1985;45:3668–76.
17. Yoneda J, Kuniyasu H, Crispens MA, Price JE, Bucana CD, Fidler IJ. Expression of angiogenesis-related genes and progression of human ovarian carcinomas in nude mice. J Natl Cancer Inst 1998;90:447–54.
18. Langley RR, Ramirez KM, Tsan RZ, Van Arsdall M, Nilsson MB, Fidler IJ. Tissue-specific microvascular endothelial cell lines from H-2K(b)-tsA58 mice for studies of angiogenesis and metastasis. Cancer Res 2003;63:2971–6.
19. Zarei S, Frieden M, Rubi B, Villemin P, Gauthier BR, Maechler P, et al. Dopamine modulates von Willebrand factor secretion in endothelial cells via D2-D4 receptors. J Thromb Haemost 2006;4:1588–95.
20. Han HD, Mangala LS, Lee JW, Shahzad MM, Kim HS, Shen D, et al. Targeted gene silencing using RGD-labeled chitosan nanoparticles. Clin Cancer Res 2010;16:3910–22.

21. Landen CN Jr, Lu C, Han LY, Coffman KT, Bruckheimer E, Halder J, et al. Efficacy and antivascular effects of EphA2 reduction with an agonistic antibody in ovarian cancer. J Natl Cancer Inst 2006;98: 1558–70.

22. Sood AK, Bhatty R, Kamat AA, Landen CN, Han L, Thaker PH, et al. Stress hormone-mediated invasion of ovarian cancer cells. Clin Cancer Res 2006;12:369–75.

23. Landen CN, Merritt WM, Mangala LS, Sanguino AM, Bucana C, Lu C, et al. Intraperitoneal delivery of liposomal siRNA for therapy of advanced ovarian cancer. Cancer Biol Ther 2006;12:1708–13.

24. Lu C, Han HD, Mangala LS, Ali-Fehmi R, Newton CS, Ozbun L, et al. Regulation of tumor angiogenesis by EZH2. Cancer Cell 2010;18: 185–97.

25. Spannuth WA, Nick AM, Jennings NB, Armaiz-Pena GN, Mangala LS, Danes CG, et al. Functional significance of VEGFR-2 on ovarian cancer cells. Int J Cancer 2009;124:1045–53.

26. Missale C, Nash SR, Robinson SW, Jaber M, Caron MG. Dopamine receptors: from structure to function. Physiol Rev 1998;78:189–225.

27. Civelli O. Molecular Biology of the Dopamine Receptor Subtypes. Philadelphia, PA: Lippincott Williams & Wilkins; 1995.

28. Best J, Nijhout HN, Reed MC. Homoestatic mechanisms in dopamine synthesis and release: a mathematical model. Theor Biol Med Model 2009;6:21.

29. Birtwistle J, Baldwin D. Role of dopamine in schizophrenia and Parkinson's disease. Br J Nurs 1998;7:832–4.

30. Mortensen PB. The incidence of cancer in schizophrenic patients. J Epidemiol Community Health 1989;43:43–7.

31. Goldacre M, Kurina L, Wotton C, Yeates D, Seagroatt V. Schizophrenia and cancer: an epidemiological study. Br J Psychiatry 2005;187: 334–8.

32. Asada M, Ebihara S, Numachi Y, Okazaki T, Yamanda S, Ikeda K, et al. Reduced tumor growth in a mouse model of schizophrenia lacking the dopamine transporter. Int J Cancer 2008;123:511–8.

33. Basu S, Dasgupta PS. Role of dopamine in malignant tumor growth. Endocrine 2000;12:237–41.

34. Sarkar C, Chakroborty D, Mitra RB, Banerjee S, Dasgupta PS, Basu S. Dopamine in vivo inhibits VEGF-induced phosphorylation of VEGFR-2, MAPK, and focal adhesion kinase in endothelial cells. Am J Physiol Heart Circ Physiol 2004;287:H1554–60.

35. Perez-Lloret S, Bondon-Guitton E, Rascol O, Montastruc JL. Adverse drug reactions to dopamine agonists: a comparative study in the French Pharmacovigilance Database. Mov Disord 2010;25: 1876–80.

36. Perez-Lloret S, Rascol O. Dopamine receptor agonists for the treatment of early or advanced Parkinson's disease. CNS Drugs 2010;24: 941–68.

37. Kerr JL, Timpe EM, Petkewicz KA. Bromocriptine mesylate for glycemic management in type 2 diabetes mellitus. Ann Pharmacother 2010;44:1777–85.

38. McGrath BP. Dopamine: clinical applications iii. Cardiovascular. Aust Prescriber 1994;17:44–5.

39. Bankowski BJ, Zacur HA. Dopamine agonist therapy for hyperprolactinemia. Clin Obstet Gynecol 2003;46:349–62.

40. Schettini G, Lombardi G, Merola B, Colao A, Miletto P, Caruso E, et al. Rapid and long-lasting suppression of prolactin secretion and shrinkage of prolactinomas after injection of long-acting repeatable form of bromocriptine (Parlodel LAR). Clin Endocrinol 1990;33:161–9.

41. Han LY, Landen CN, Trevino JG, Halder J, Lin YG, Kamat AA, et al. Antiangiogenic and antitumor effects of SRC inhibition in ovarian carcinoma. Cancer Res 2006;66:8633–9.

42. Boyd DD, Wang H, Avila H, Parikh NU, Kessler H, Magdolen V, et al. Combination of an SRC kinase inhibitor with a novel pharmacological antagonist of the urokinase receptor diminishes in vitro colon cancer invasiveness. Clin Cancer Res 2004;10:1545–55.

43. Eliceiri BP, Paul R, Schwartzberg PL, Hood JD, Leng J, Cheresh DA. Selective requirement for Src kinases during VEGF-induced angiogenesis and vascular permeability. Mol Cell 1999;4:915–24.

44. Bhattacharya R, Sinha S, Yang SP, Patra C, Dutta S, Wang E, et al. The neurotransmitter dopamine modulates vascular permeability in the endothelium. J Mol Signal 2008;3:2187.